Eur. Phys. J. D **16**, 329–332 (2001)

THE EUROPEAN PHYSICAL JOURNAL D

EDP Sciences
© Società Italiana di Fisica
Springer-Verlag 2001

Coalescence process of monodispersed Co cluster assemblies

D.L. Peng[1,3,a], T.J. Konno[2], K. Wakoh[2], T. Hihara[3], and K. Sumiyama[3]

[1] CREST of Japan Science and Technology Corporation, Kawaguchi 332-0012, Japan
[2] Institute for Materials Research, Tohoku University, Sendai 980-8577, Japan
[3] Department of Materials Science and Engineering, Nagoya Institute of Technology, Nagoya 466-8555, Japan

Received 29 November 2000

Abstract. Cluster-cluster coalescence process of monodispersed Co clusters with mean diameter $d = 8.5$ and 13 nm deposited a plasma-gas-condensation-type cluster beam deposition system was investigated by *in situ* electrical conductivity measurements and *ex situ* scanning electron microscopy (SEM) and transmission electron microscopy (TEM), and analyzed by percolation concept. The electrical conductivity measurement and TEM observation indicated that, below temperature $T \approx 100$ °C, the Co clusters in the assemblies maintain their original structure as deposited at room temperature, while that the inter-cluster coalescence takes place at $T > 100$ °C, although the size distribution and the interface morphology of the clusters showed no marked change at substrate temperatures $T_s \leq 200$ °C.

PACS. 61.46.+w Nanoscale materials: clusters, nanoparticles, nanotubes, and nanocrystals – 73.40.-c Electronic transport in interface structures – 61.16.Bg Transmission, reflection, and scanning electron microscopy

1 Introduction

A cluster-assembling method [1], in which nanometer-sized clusters are directly deposited on a substrate, is a promising alternative to fabricate ideally-controlled nanoscale materials. Throughout the assembling process, it is desirable to maintain the initial size and structure of the clusters. In practice, however, interaction among the deposited clusters takes place on a substrate, preventing one from achieving this goal. This interaction is known to depend on several factors: deposited materials, cluster size, substrate temperature and contamination. Considering the potential application of the Co cluster assembly, it is necessary to explore the clusters-cluster coalescence process above the room temperature. Recently, using a plasma-gas-condensation (PGC) type cluster deposition apparatus, we have succeeded in preparing monodispersed Co clusters with the mean sizes $d = 6$ to 15 nm. In this report, we describe coalescence behaviors of the Co cluster assemblies obtained by *in situ* electrical resistivity measurement and *ex situ* SEM and TEM observation.

2 Experimental

Co clusters were prepared by the PGC-type cluster beam deposition apparatus [2–4], which is based on plasma-glow-discharge vaporization (sputtering) and inert gas condensation techniques [5]. The apparatus is composed of the three main parts: a sputtering chamber, a cluster growth room and a deposition chamber. The vaporized atoms in the sputtering chamber are decelerated by collisions with a large amount of Ar gas injected continuously into the sputtering chamber (the Ar gas flow rate: $R_{\mathrm{Ar}} = 250-500$ SCCM), and are swept into the cluster growth room, which is cooled by liquid nitrogen. The clusters formed in this room are ejected from a small nozzle by differential pumping and a part of the cluster beam is intercepted by a skimmer, and then deposited onto a substrate, which can be heated up to 500 °C by a resistive heater and is fixed on the sample holder in the deposition chamber. We used two kinds of substrates for the Co cluster deposition: TEM microgrids for TEM observations and quartz plates with two pre-coated Au electrodes (4 mm width and 1 mm separation) for *in situ* electrical resistivity measurements. The effective Co-cluster-assembled film thickness of deposited clusters, t, was estimated using a crystal quartz thickness monitor, which measures the weight of the deposited clusters. We carried out *in situ* measurement of electrical conductivity in the deposition chamber with a vacuum of about 1×10^{-6} torr. Using a constant current mode, the voltage change between two electrodes was detected with a digital voltmeter as a function of the temperature.

[a] e-mail: pengdl@mse.nitech.ac.jp

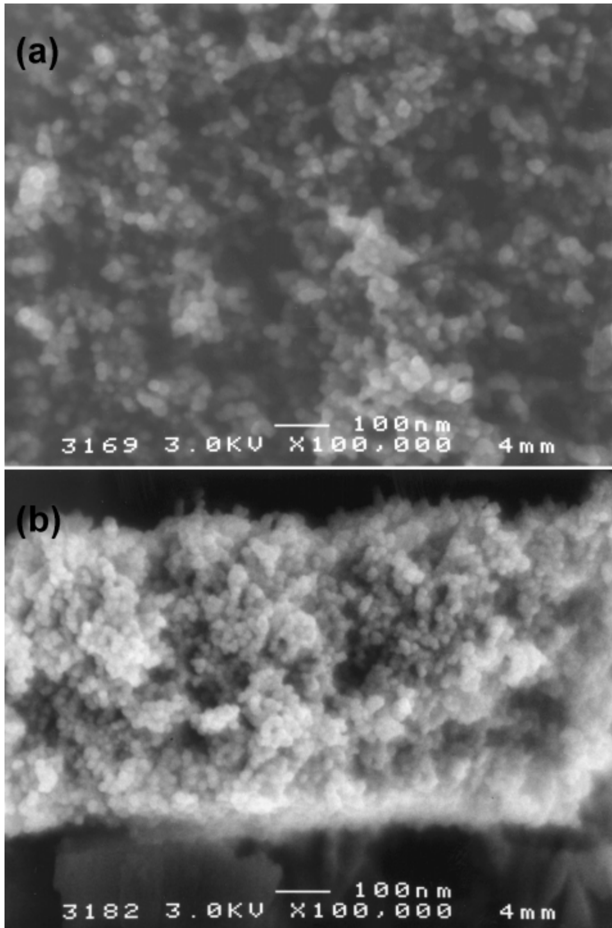

Fig. 1. Plan-view and cross-sectional SEM images of the Co-cluster-assembled film with the mean cluster diameter, d = 13 nm. The effective thickness of the deposited film is 150 nm.

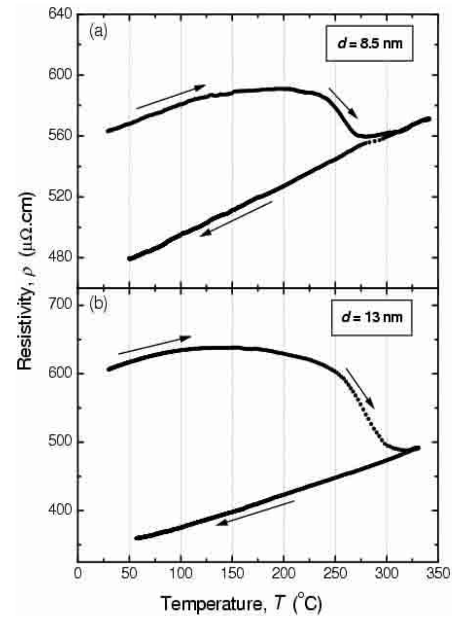

Fig. 2. *In situ* electrical resistivity ρ as a function of temperature T for the Co monodispersed cluster assemblies with $d = 8.5$ and 13 nm, and $t = 300$ nm deposited on the quartz substrates at room temperature, where the heating rate is 10 °C min^{-1}. The arrows show the increase and decrease directions of temperature.

3 Results and discussion

We observed the morphology of the Co cluster deposited film with a high resolution SEM (JEOL: JSM-6320F) operating at 3 kV. Figures 1(a) and 1(b) show the plan-view and cross-sectional SEM images of the Co-cluster-assembled film with $d = 13$ nm. The plan-view image reveals very bumpy film surfaces containing inhomogeneous aggregations of the Co clusters. In the cross-sectional image, we observe a random stacking of the Co clusters but detect no columnar structure (texture) as has been observed in the films deposited by conventional thermal evaporation and sputtering. In both images, individual Co clusters are distinguishable. This suggests that the Co clusters in the assemblies maintain their original size at room temperature. Moreover, the film thickness estimated from the cross-sectional SEM image is about $t = 540$ nm, although the planned film thickness was $t = 150$ nm. This implies that the cluster assemblies are very porous.

Figures 2(a) and 2(b) show the electrical resistivity ρ as a function of temperature T for the Co monodispersed cluster assemblies deposited on the quartz substrate at room temperature with $d = 8.5$ and 13 nm, where $t = 300$ nm. The heating rate is 10 °C min^{-1}. As can be seen from Fig. 1, the temperature dependence of ρ reveals an irreversible behavior, being divided into three distinct stages in temperature-rising curve. At first, below 100 °C, ρ linearly increases with increasing T and shows ordinary metallic temperature dependence. This is well correlated with the result [6] obtained in the temperature range of 4.2-300 K: it showed the residual resistance at low temperatures and a linear increase with increasing T. Secondly, at $100 < T < 200$ °C, ρ still shows a gradual increase with temperature, but its increase rate clearly deviates from the linear behavior, until finally it starts to decrease slowly with increasing T. This observation strongly suggests that the Co clusters starts to electrically contact each other and the cluster-cluster coalescence takes place in this temperature range. Finally, above 200 °C, ρ decreases dramatically with increasing T, and then exhibits a minimum at T_M, which we call the reversible transition temperature. When $T > T_M$, the resistivity exhibits once again the ordinary metallic temperature dependence and coincides with that in the temperature-lowering curve, resulting in the reversible behavior. Our experimental result also indicated that T_M depends on the cluster size and is shifted to the high temperature region with increasing the cluster size. This observation implies that small clusters can coalesce more easily than the large ones, probably because of size-dependent surface melting point of Co clusters. The surface melting of platinum clusters has recently been discussed by Wang [7] in the context of the treatment by Buffat and Borel [8]. Application of this analysis to the case of Co clusters suggests the plausibility of surface melting near 300 °C.

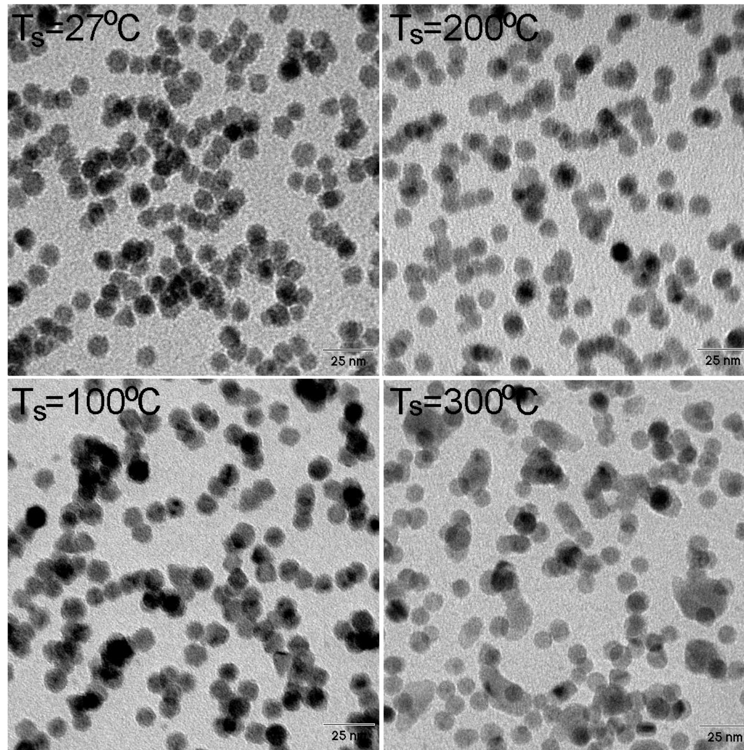

Fig. 3. Bright field TEM images of the Co clusters with d = 8.5 nm deposited on carbon-film-coated TEM microgrids as a function of the substrate temperatures T_s.

Figure 3 shows the bright field TEM images in the initial stage of the Co clusters with d = 8.5 nm produced at several substrate temperatures T_s = 27, 100, 200 and 300 °C. As shown here, at T_s = 27 °C (room temperature), the clusters are almost monodispersed even though some clusters contact and overlap each other. Moreover, the size and distribution of the clusters show no marked change up to T_s = 200 °C, though the electrical resistivity measurement reveals that the coalescence starts even as low as T = 100 °C. When T_s > 200 °C, we clearly observe the inter-cluster coalescence and the growth of the combined clusters, being in agreement with the behavior of the rapid decrease of the resistivity in this temperature range.

As described above, the electrical resistivity measurement and TEM observation have a difference in the temperature range of 100-200 °C on the coalescence behavior of the clusters. In fact, it is difficult to observe directly the interfacial coalescence process of the clusters by TEM. In order to further examine the coalescence behavior of the interfacial regions between the clusters touching each other, we carried out *in situ* electrical percolation (2D) measurement because the present cluster deposition process can be understood by the percolation concept [3]. Figure 4 shows the electrical conductivity, σ, as a function of t at the substrate temperatures T_s = 27, 100, 200 and 300 °C. In the initial deposition stage, σ is zero because the circuit between the two electrodes is opened: the discontinuous 2D film growth stage. At $t \approx 6.5$ nm, σ starts to increase rapidly due to the one-set of formation of continuous cluster networks between the electrodes. Using the sliding least-squares fit procedure [9], we fitted the following scaling-law to our measured data of σ near the percolation threshold:

$$\sigma \propto (t - t_c)^{\mu},$$

where the critical thickness t_c and the critical exponent μ are the fitting parameters. We plot them as a function of T_s in Figures 5(a) and 5(b). As shown in Fig. 5(b), μ exhibits no distinct substrate temperature dependence and has a value of 1.12-1.15, being consistent with the theoretical and experimental value (1.1-1.3) in the 2D percolation [10,11]. It is evident from Fig. 5(a) that the t_c value is dependent on T_s. At T_s = 100 °C, the t_c value is about the same with that at room temperature, while, above T_s = 100 °C, the t_c value increases rapidly with increasing T_s. According to the measurement results of the electrical percolation at room temperature [3], t_c increases with increasing cluster size d, owing to the partial overlapping of deposited clusters. Therefore, the rapid increase of the t_c value with T_s above T_s = 100 °C can be ascribed to coalescence and growth of the clusters touching each other, being in agreement on the result of the continuous temperature-rising electrical resistivity measurement (see Fig. 2).

4 Conclusion

We have deposited nanometer-sized Co clusters on quartz substrates with two pre-coated Au electrodes

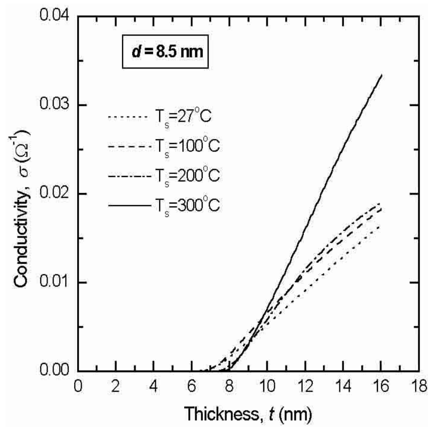

Fig. 4. Electrical conductivity, σ, *versus* effective deposition thickness, t, during the assembling process of the Co cluster ($d = 8.5$ nm) deposited on the quartz substrate at substrate temperature $T_s = 27$, 100, 200 and 300 °C.

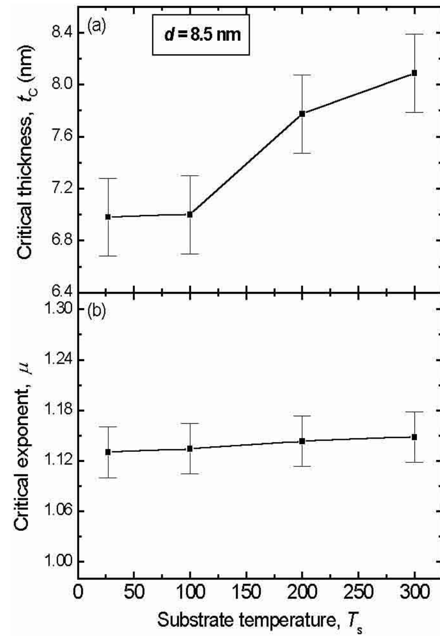

Fig. 5. (a) Critical thickness, t_c, and (b) critical exponent, μ, as a function of the substrate temperature, T_s, for Co cluster deposition on the quartz substrates.

and TEM microgrids by the plasma-gas-condensation (PGC) method. Cluster-cluster coalescence behavior of the monodispersed Co clusters was studied by electrical conductivity, SEM and TEM, and discussed by the percolation concept. The results show that, below $T \approx 100$ °C, the Co clusters in the assemblies maintain the same original size and structure as deposited at room temperature, while that the inter-cluster coalescence takes place at $T > 100$ °C.

This work has been supported by Core Reseach for Evolutional Science and Technology (CREST) of Japan Science and Technology Corporation (JST), and partly by Grnat-in-Aid for Scientific Research A1 (Grant No. 08505004). We are also indebted to the support from Laboratory for Development Reseach of Advanced Materials of IMR.

References

1. P. Melinon *et al.*, Int. J. Mod. Phys. B **9**, 339 (1995).
2. S. Yamamuro, K. Sumiyama, K. Suzuki, J. Appl. Phys. **85**, 483 (1999).
3. S. Yamamuro, K. Sumiyama, T. Hihara, K. Suzuki, J. Phys.: Cond. Matt. **11**, 3247 (1999).
4. S. Yamamuro, K. Sumiyama, T. Kamiyama, K. Suzuki, J. Appl. Phys. **86**, 5726 (1999); S. Yamamuro, K. Sumiyama, T.J. Konno, K. Suzuki, Mater. Trans. JIM **40**, 1450 (1999).
5. H. Haberland, M. Karrais, M. Mall, Y. Thurner, J. Vac. Sci. Technol. A **10**, 3266 (1992).
6. D.L. Peng, K. Sumiyama, S. Yamamuro, T. Hihara, T.J. Konno, Phys. Rev. B **60**, 2093 (1999).
7. Z.L. Wang, J.M. Petroski, T.C. Green, M.A. El-Sayed, J. Phys. Chem. B **102**, 6145 (1998).
8. Ph. Buffat, J.-P. Borel, Phys. Rev. A **13**, 2287 (1976).
9. L. Cheriet, H.H. Helbig, S. Arajs, Phys. Rev. B **39**, 9828 (1989).
10. A.B. Harris, Phys. Rev. B **28**, 2614 (1983).
11. J.A.J. Lourens, S. Arajs, H.F. Helbig, El-Sayed, A. Mehanna, L. Cheriet, Phys. Rev. B **37**, 5423 (1988).